American Journal of BioMedicine
AJBM 2015;3(1): 423–439
Research Article doi: 10.18081/2333-5106/015-01/339-356

Tpl2 exaggerated ischemic hepatic injury through induction of apoptosis: Downstream of caspase-9

Douglas H Jacob, Ingrid U Zeng, Yukio Tsung, Shao-Ling Qin, Levi R Blair, Chris A Clarkson, Michael T Braun, Mao Zhao*

Abstract

Ischemia-reperfusion injury is a dynamic process that involves the two interrelated phases of local ischemic insult and inflammation-mediated reperfusion injury, and an important cause of liver damage occurring during surgical procedures and represents the main underlying cause of graft dysfunction post-transplantation. This study is a highlight into innate-adaptive immune crosstalk and cell activation cascades that lead to inflammation-mediated injury in livers stressed by ischemia-reperfusion. Tumor Progression Locus 2 (TPL2) is a serine-threonine kinase with essential functions in innate immune cells, where it transmits signals through Toll-like receptors family. To explore the role of Tpl2 in hepatic injury, liver ischemia/reperfusion injury was induced in wild type mice (Tpl2+/+) and in Tpl2-/- mice. They were sacrificed after 3-days post I/R. We determined TPL2 mRNA levels by quantitative PCR (qPCR), DNA and total RNA extraction from tissues was performed using the DNeasy and miRNeasy Kits, the extents of liver and function were studied. Tpl2 knockout mice produce low levels of proinflammatory cytokines expression, reduced release of LDH, ALT and less hepatic injury than wild type mice when exposed to I/R. Interestingly caspase-3 activation was significantly lower in Tpl2-/- mice. These results suggested that Tpl2 directly involved in apoptotic signal at the level of caspase-3 activation downstream of caspase-9, and that Tpl2 contributed to the exaggerated of ischemic liver injury through induction of apoptosis.

Keywords: Tpl2; Liver I/R; Caspase-3; Caspase-9; Proinflammatory cytokines

*Corresponding author email: MaoZ@uni.mis.edu
[1]Department of Gastroenterology, University of Mississippi Medical Center, United States
Received 30 November 2014; accepted February 22, 2015, Published March 14, 2015

Introduction

Liver's function in the body as both a filter for toxins and an innate immune organ, the liver is predisposed to cellular turnover. Under healthy conditions, this occurs through the removal of aging and damaged hepatocytes by apoptosis. However, in a diseased liver, pathological cell death often occurs. In the previous twenty years, there has been considerable discussion in the research community over the different types of cell death [1].

Research Article doi: 10.18081/2333-5106/015-01/339-356

Apoptosis has a complex signaling pathway that prototypically results in activation of caspases in hepatocytes, resulting in the degradation of cellular proteins and activation of DNases, which cleave nuclear DNA, and induce cell death. As such, inhibition of caspases has routinely been tested in multiple models of liver disease as a potential means for reducing cell death. However, caspase inhibitors have failed to protect in many of these experiments [2].

One reason discussed extensively was the fact that apoptosis was not the major mode of cell death in these models [3]. In addition, recent studies have indicated caspase inhibition can have profound effects outside of just inhibition of apoptotic cell death and may not always interrupt the cell death process in a sustainable fashion.

Nomenclature in the literature refers to apoptotic cell death and necrotic cell death in diseased livers. Apoptosis is defined morphologically on the basis of cellular rounding up, cytoplasmic shrinkage (pyknosis), chromatin condensation, and nuclear fragmentation (karyorrhexis). Effector caspase (proteases that cleave at aspartate residues) activation is required for the acquisition of this morphology. Necrotic cell death has the morphology of oncosis (cell swelling due to the inability to maintain cellular ion gradients), karyolysis, and rupture of the plasma membrane [4].

While definitions are useful as broad categories, understanding the minute mechanisms that lead to cell death and ensuing injury are more important than allotting modes of cell death to a particular liver disease [5]. Suffice it to say that in the liver, morphologically observed cell death can be apoptotic or necrotic or a combination of the two. Furthermore, the same stimulus can result in either morphology [6]. It is conceivable that on a cellular basis, necrosis in the liver is the result of overwhelming or dysregulated apoptosis.

For example, exaggerated mitochondrial dysfunction from “apoptotic” signaling cascades can result in cellular adenosine triphosphate depletion and necrotic morphology. Hepatocytes are the most numerous cell type in the liver, and their apoptosis is prominent in liver injury.3–5 Councilman bodies, described by the pathologist William T. Councilman (1854 – 1933), in the liver of patients with yellow fever result from apoptotic death of individual hepatocytes [7]. On careful examination, hepatocyte apoptosis can be identified in virtually all forms of liver injury [8]. Apoptosis of other cellular compartments is also important. For example, sinusoidal endothelial cell apoptosis is observed in ischemia-reperfusion injury, and failure of activated stellate cell apoptosis promotes fibrosis [9].

The M30 neoantigen is one example of an emerging clinical applicability of the apoptosis cascade [10]. This epitope is formed by proteolytic cleavage of cytokeratin 18 by caspase 3 at Asp396 position. It is readily detectable in plasma by enzyme-linked immunosorbent assay. Circulating levels are increased in patients with chronic liver disease, and highest levels are found in patients with cholestasis or cholangitis [11]. Levels in hepatic graft-versus-host disease are elevated and correlate with response to therapy.13 In patients with steatohepatitis, serum levels of M30 correlate with liver levels and inflammation [12]. Thus, a biomarker reflecting hepatocyte apoptosis may eventually be important in establishing and monitoring therapy in

Research Article doi: 10.18081/2333-5106/015-01/339-356

human liver diseases. The appearance of serum cytokeratin 18 degradation products in virtually all liver diseases also highlights the role of caspases in liver tissue injury. Apoptosis can be initiated from any membrane-defined organelle in the cell. In this review, we emphasize this mechanistic concept [13-16].

Methods and materials

injury model in mice

Tpl2+/+ and tpl2−/− mice (C57BL/6 background) are described previously [17] and C57BL/6-CD1d−/− mice were purchased from The Jackson Laboratory (Bar Harbor, ME). Tpl2+/− animals were used to generate experimental groups of different tpl2 genotypes, which were cohoused and maintained in identical conditions prior to treatments. To induce immune-mediated hepatitis, 8- to 10-wk-old female mice were injected i.v. with Con A (Sigma-Aldrich) at a dose of 10 mg/kg body weight and were euthanized at the indicated time points after Con A treatment. For the assessment of the effects of kinase inhibition, a TPL2 inhibitor (Calbiochem) dissolved in DMSO was administered i.p. at a dose of 250 μg/mouse 15 h and 30 min before Con A treatment, whereas the control animals received equal amount of DMSO. To induce NKT cell–mediated liver injury, mice received 100 μg/kg α-galactocylceramide (αGalCer, KRN7000; Enzo Life Sciences) for the indicated time points. Control mice of all study groups received PBS as control.

Histology

For histopathology, liver tissue sections were excised at various time points, fixed overnight in 10% neutral formalin solution, and embedded in paraffin. Sections of 5 μM were prepared, placed on glass lesions, and stained with H&E to assess liver injury. To assess the extent of apoptotic areas, liver tissue was stained for activated caspase-3. Inactivation of endogenous peroxidase was achieved by incubating the deparaffinized sections with hydrogen peroxide/methanol. Ag retrieval was performed by using 10 mM sodium citrate buffer (pH 6). Sections were blocked using an Avidin/Biotin Kit (Vector Laboratories), followed by addition of 20% pig serum in PBS.

A primary Ab was used against caspase-3 (CS9664; Cell Signaling Technology) at a 1:200 dilution in PBS, followed by overnight incubation at 4°C. Sections were washed and further incubated with biotinylated swine anti-rabbit at 1:200 (DakoCytomation) for 1 h and washed, and immunohistochemistry was completed with streptavidin biotin–peroxidase complex incubation (Vector Laboratories) for 45 min. Caspase-3–positive cells were visualized by 3,3′-diaminobenzidine tetrahydrochloride, and sections were hematoxylin counterstained. Morphometric image analysis was performed using Leica QWin software

Research Article doi: 10.18081/2333-5106/015-01/339-356

Flow cytometry

For flow cytometric analysis, cells were resuspended in 100 µl FACS buffer (PBS containing 5% FBS). For extracellular markers, single-cell suspensions of LMNCs were stained with specific fluorescently conjugated Abs for 30 min at 4°C in the dark. The following Abs were used from eBioscience: CD3 (clone 145-2C11), NK1.1 (clone PK136), CD69 (clone H1.2F3), CD4 (clone RM4-5), CD8 (clone 53-6.7), Gr1 (clone; RB6-8C5), CD11b (clone; M1/70), CD11c (clone N418), CD19 (clone MB19-1), CD24 (clone 30-F1), CD44 (clone IM7), and IL-4 (clone BVD6-24G2).

For tetramer staining, LMNCs (2 × 106 cells) were preincubated for 10 min with anti-CD16/32 for blocking of FcRs and labeled with appropriate dilutions of PE-conjugated CD1dPBS57-tetramer for 45 min at 4°C in the dark. Cells were washed and resuspended in PBS/5% FBS. For IL-4 intracellular staining, DN32.D3 cells were treated with 200 ng/ml αGalCer in the presence or absence of TPL2 inhibitor. Secretion of cytokines was blocked by either momensin or brefeldin A protein transport inhibitors (eBioscience). Cells were stained with cell surface markers and then fixed and permeabilized with eBioscience fixation and permeabilization buffers, according to the manufacturer's intracellular staining protocol. Flow cytometric analysis was performed and acquired on a FACSCalibur (BD Biosciences), and data were analyzed using the FlowJo software (Tree Star).

Cell sorting and NKT:DC coculture

The TCRβ$^+$CD1d tetramer$^+$ NKT cell population and CD11c$^+$ dendritic cells (CD11c$^+$ DCs) were sorted from LMNCs of *tpl2*$^{+/+}$ *and* *tpl2*$^{-/-}$ mice using the high-speed cell sorter MoFlo (DakoCytomation). *Tpl2*$^{+/+}$ and *tpl2*$^{-/-}$CD11c$^+$ DCs (purity > 90%) were treated with αGalCer to the final concentration 100 ng/ml for 18 h. *Tpl2*$^{+/+}$ and *tpl2*$^{-/-}$ αGalCer–pulsed DCs were cocultured with purified *tpl2*$^{+/+}$ and *tpl2*$^{-/-}$ NKT cells (purity > 95%) in all possible combinations at ratio 1:2 for 24 h. Coculture supernatants were collected and analyzed for IL-4 and IFN-γ secretion.

NKT cell isolation and adoptive transfer

LMNCs were isolated from *tpl2*$^{+/+}$ and *tpl2*$^{-/-}$ mice as described above. NKT cells were enriched from hepatic MNCs by magnetic cell sorting (130-096-513; Miltenyi Biotec). In brief, CD3-positive cells were enriched by negative selection (MACS), according to the manufacturer's protocol. CD3-enriched cells were stained with NK1.1 APC mAb and incubated with anti-APC microbeads, and NK1.1-positive cells were enriched by positive magnetic cell sorting according to the manufacturer's recommendations. Approximately 90% of the magnetic cell sorting–purified cells were CD3 and NK1.1 positive. Purified *tpl2*$^{+/+}$ or *tpl2*$^{-/-}$ NKT cells (0.5 × 10^6) were injected i.v. into CD1d-deficient mice, respectively. Con A was injected at a dose of 10 mg/kg,

Research Article doi: 10.18081/2333-5106/015-01/339-356

mice were then euthanized 8 h postinjection, and their sera and livers were analyzed. Liver injury was assessed by measuring serum levels of ALT/AST transaminases.

ELISA

Cytokine concentration in serum and cell culture supernatants was determined by ELISA at the indicated time points using ELISA kits for mouse IL-4, IFN-γ, TNF, IL-6, IL-2, and IL-12 (all purchased by eBioscience), according to the manufacturer's instructions. Colorimetric reactions were stopped by the addition of 1 N HCl, and the optical absorbance at 450 and 570 nm was determined using a microplate absorbance reader (Model 680 Microplate Reader; Bio-Rad).

Quantitative PCR expression assay

RNA was isolated from NKT hybridoma cell line DN32.D3 or liver tissue using TRIzol (Invitrogen) and Nucleospin RNA kit (MACKEREY-NAGEL), respectively. Total RNA was quantified with a Nanodrop Spectrophotometer. A High-Capacity cDNA Reverse Transcription kit was used to synthesize cDNA from 500 ng RNA, according to the manufacturer's protocol using the High-Capacity cDNA Archive kit (Applied Biosystems).

Applied Biosystems TaqMan Universal PCR Mastermix and TaqMan gene expression probes for mouse IL-4 (Mm00445259_m1, FAM labeled), IFN-γ (Mm01168134_m1, FAM-labeled), GATA-3 (Mm00484683_m1, FAM labeled), MAF (Mm02581355_s1, FAM-labeled), T-bet (Mm00450960_m1, FAM-labeled), Fas ligand (Mm00438864_m1, FAM-labeled), JunB (Mm04243546_s1, FAM-labeled), CXCL1 (Mm04207460 _m1, FAM-labeled), CXCL2 (Mm00436450_m1), CCL3 (Mm00441259_g1, FAM-labeled), and β-actin (ACTB; Mm00607939_s1) as endogenous control (VIC-labeled) were obtained from Applied Biosystems and used on an Applied Biosystems ViiA Real-Time PCR Instrument.

All assays were run in duplicate on an Applied Biosystems ViiA Real-Time PCR system, according to the manufacturer's instructions, and the mean value was used for the analysis. mRNA levels were expressed as relative quantification (RQ) values, which were calculated as $RQ = 2^{(-\Delta\Delta Ct)}$, where ΔCt is (Ct [gene of interest] − Ct [housekeeping gene]).

Protein isolation

Following treatment, cells or liver tissues were lysed in radioimmunoprecipitation assay buffer, containing 50 mM Tris-HCl (pH 7.4), 150 mM NaCl, 1% Nonidet P-40, 0.5% sodium deoxycholate, 0.1% SDS, protease inhibitors (Sigma-Aldrich), 100 mM Na_3VO_4 (Sigma-Aldrich), and 1 mM NaF (Sigma-Aldrich). For Western blot analysis, levels of total proteins were determined using the bicinchoninic acid assay (Thermo-Scientific).

For fractionation of cytoplasmic and nuclear protein extracts, cells were lysed in buffer A (10 mM HEPES [pH 7.9], 10 mM KCl, 0.1 mM EDTA, and 10% Nonidet P-40) supplemented with protease inhibitors and 100 mM Na_3VO_4 and 1 mM NaF. Lysates were rotated on a platform for 15 min at 4°C, and the cytosolic fraction was purified by centrifugation at 13,000 rpm at 4°C for 4 min. The pellet of nuclei was resuspended in buffer B (20 mM HEPES [pH 7.9], 0.4 M NaCl,

0.1 mM EDTA, 10% glycerol, protease inhibitors, 100 mM Na_3VO_4, and 1 mM NaF), and extracts were incubated on ice for 30 min. The nuclear fraction was purified by centrifugation at 13,000 rpm at 4°C for 4 min.

Cytoplasmic and nuclear protein concentration was measured using the Bio-Rad DC protein assay kit. An amount of 30 μg/sample was loaded and subjected to SDS-PAGE and subsequently transferred to a nitrocellulose membrane (Whatman) following blocking with 5% nonfat milk in TBS-T before incubation with primary Ab.

The following Abs were used for immunoblotting: p-ERK1/2 (CS4370; Cell Signaling Technology), pp38 (CS4511; Cell Signaling Technology), pJNK1/2 (CS4668; Cell Signaling Technology), pAKT (CS4060; Cell Signaling Technology), pGSK3β-Ser9 (CS5558; Cell Signaling Technology), pSTAT1 (CS9171; Cell Signaling Technology), pSTAT3 (CS9131; Cell Signaling Technology), pSTAT6 (CS9361; Cell Signaling Technology), ERK1/2 (CS4695; Cell Signaling Technology), p38 (CS8690; Cell Signaling Technology), JNK1/2 (CS9258; Cell Signaling Technology), AKT (CS2920; Cell Signaling Technology), STAT1 (610115, BD Transduction Laboratories.), STAT3 (CS9132; Cell Signaling Technology), STAT6 (CS9362; Cell Signaling Technology), NFATc1 (CS5861; Cell Signaling Technology), Sp1 (PEP-2; Santa Cruz Biotechnology), TPL2 (M-20; Santa Cruz Biotechnology), IκBα (CS4814; Cell Signaling Technology), p-IκB kinase (IKK)α/β (CS2697; Cell Signaling Technology), IKKβ (CS8943; Cell Signaling Technology), and β-actin (clone X-4; Millipore). Secondary HRP-conjugated Abs were purchased by Sigma-Aldrich and used at a concentration of 1:20,000. ECL method (PerkinElmer Life Sciences) was used for signal development.

NKT cell isolation and adoptive transfer

LMNCs were isolated from *tpl2*$^{+/+}$ and *tpl2*$^{-/-}$ mice as described above. NKT cells were enriched from hepatic MNCs by magnetic cell sorting (130-096-513; Miltenyi Biotec). In brief, CD3-positive cells were enriched by negative selection (MACS), according to the manufacturer's protocol. CD3-enriched cells were stained with NK1.1 APC mAb and incubated with anti-APC microbeads, and NK1.1-positive cells were enriched by positive magnetic cell sorting according to the manufacturer's recommendations.

Approximately 90% of the magnetic cell sorting–purified cells were CD3 and NK1.1 positive. Purified *tpl2*$^{+/+}$ or *tpl2*$^{-/-}$ NKT cells (0.5×10^6) were injected i.v. into CD1d-deficient mice, respectively. Con A was injected at a dose of 10 mg/kg, mice were then euthanized 8 h postinjection, and their sera and livers were analyzed. Liver injury was assessed by measuring serum levels of ALT/AST transaminases.

Cell culture and treatments

Primary murine LMNCs and splenocytes were cultured in RPMI 1640 supplemented with 10% FBS, 1% nonessential amino acids, 1% penicillin-streptomycin, 1% sodium pyruvate, and 50 μM 2-ME (all purchased by Life Technologies) and treated with 100 ng/ml with αGalCer at the indicated time points. The Va14$^+$ CD1d-specific NKT hybridoma cell line DN32.D3 was a gift

Research Article doi: 10.18081/2333-5106/015-01/339-356

from Dr. A. Bendelac (University of Chicago, Chicago, IL). DN32.D3 cells were maintained in hybridoma medium consisted of RPMI 1640 supplemented with EHAA (Sigma-Aldrich), 10% FBS, 1% penicillin-streptomycin, 1% l-glutamine (Sigma-Aldrich), gentamicin (Sigma-Aldrich), and 50 μM 2-ME (Life Technologies). Cells were treated with DMSO (Applichem) as vehicle control, 5 μM TPL2 kinase inhibitor (Calbiochem, Merck-Millipore), 5 μM UO126 (Calbiochem, Merck-Millipore), or 0.5 μM wortmannin (Calbiochem, Merck-Millipore) 30 min before stimulation with 200 ng/ml αGalCer for various time points. In another set of experiments, cells were treated with 10 μg/ml purified anti-mouse IL-4 or/and 10 μg/ml purified anti-mouse IFN-γ and were stimulated or not with 200 ng/ml αGalCer for further analysis.

Statistical Analysis

Values are expressed as the mean ± standard error. Statistical analysis was performed using an unpaired *t* test (for two groups only) and analysis of variance (for more than two groups). Statistical significance was considered at $P < 0.05$. Calculations were made with SigmaStat 3.5 (Systat Software Inc., San Jose, CA, United States).

Results

TPL2 influences immune cell content and activation status in the liver during Con A–induced fulminant hepatitis

The pathogenesis of Con A–induced hepatitis critically depends on T and NKT cells [18]. To dissect the cellular mechanisms underlying the aforementioned pathogenic TPL2 effect, we analyzed T cell content and activation status in LMNCs isolated from WT and *tpl2*$^{-/-}$ mice during disease progression. This analysis demonstrated progressive accumulation of CD3^{+} and CD4^{+} T (Fig. 1) in Con A–treated WT mice, which was similar to that observed in *tpl2*$^{-/-}$ animals. Simultaneous assessment of the early activation marker CD69 also showed absence of significant differences in the activation status of CD3^{+} and CD4^{+} lymphocytes between strains (Fig. 1), indicating that conventional T cells are not the primary target of the TPL2 effect on Con A–induced liver injury.

Research Article doi: 10.18081/2333-5106/015-01/339-356

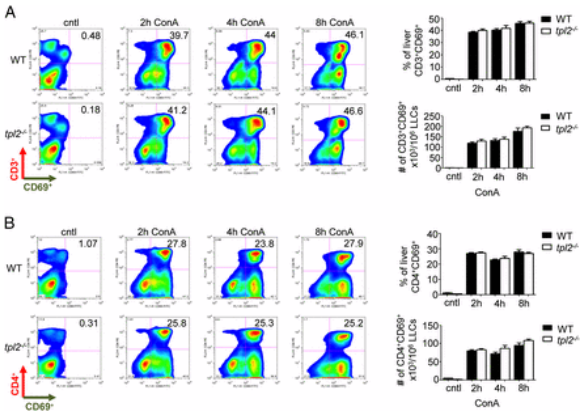

Figure 1.

TPL2 does not affect CD3 and CD4 T cell activation and infiltration during Con A–induced liver injury. (**A**) LMNCs isolated from the liver of WT and *tpl2*$^{-/-}$ mice were analyzed by flow cytometry following treatment with Con A. Representative analysis of kinetics and frequency of activated T cells as defined by CD3^{+}CD69^{+} coexpression (gated in liver lymphocytes) during the onset and the progression of immune-mediated liver damage. (*n* = 8–10 mice per group).

TPL2 ablation ameliorates immune-mediated liver injury

The physiological role of TPL2 in immune-mediated liver injury was explored using an established mouse model of fulminant hepatitis-like pathology induced by Con A [19]. Wild-type (WT; *tpl2*$^{+/+}$) and TPL2-deficient (*tpl2*$^{-/-}$) mice were administered Con A i.v., and disease severity was monitored over time. WT animals progressively developed congestive livers characterized by increased blood accumulation (Fig. 2A), histological manifestations of extensive tissue damage (Fig. 2B), and elevated expression of cleaved caspase-3 (Fig. 1C, 1D). Strikingly, *tpl2*$^{-/-}$ mice exposed to Con A displayed reduced macroscopic and histological features of liver injury (Fig. 2A–D). The serum levels of ALT and AST, which represent biochemical markers of hepatic injury (Fig. 2E) and of the proinflammatory cytokines TNF-α and IL-6 (Supplemental Fig. 2A) as markers of systemic effects, were also significantly reduced in *tpl2*$^{-/-}$ compared with WT mice treated with Con A. Con A also led to accumulation of TPL2 mRNA and protein levels in the liver of WT animals (Fig. 2F, 1G).

Research Article doi: 10.18081/2333-5106/015-01/339-356

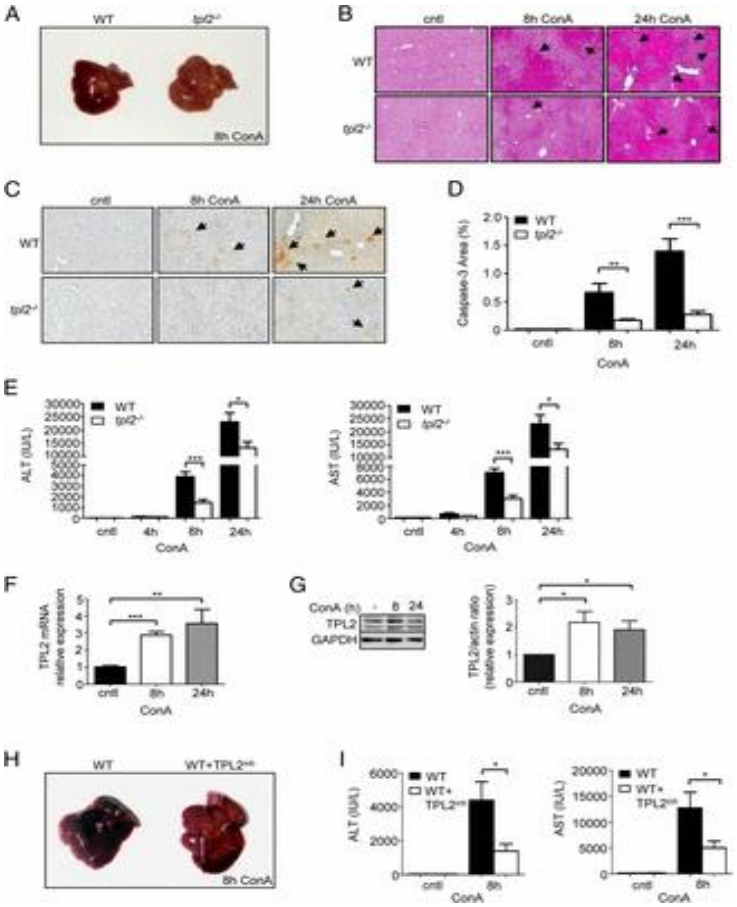

Figure 2

TPL2 kinase promotes immune-mediated liver injury. (A) Representative images of livers of WT and tpl2−/− mice treated with 10 mg/kg Con A for 8 h showing macroscopic signs of severe and mild liver injury, respectively. (B) Histopathological examination of Con A–induced liver injury following H&E staining of liver (C) Representative (n = 8) immunohistochemical analysis of cleaved caspase-3 levels in livers from WT and tpl2−/− mice treated with saline or Con A for 8 and 24 h.

The il4 and ifng-regulating transcription factors JunB and NFAT are targets of TPL2-transduced signals

Transcriptional activation of the IL-4 gene in T cells is orchestrated by GATA3-mediated chromatin remodeling, which enables binding of c-Maf and NFAT:AP1 to the *il4* promoter. NFAT is activated by TPL2 overexpression [20-24], but whether it is a physiological target of TPL2 remains unknown. JunB is a component of the NFAT:AP-1 transcriptional complex that regulates *il4* transactivation in mouse T cells [25], is upregulated in αGalCer-stimulated iNKT cells, and required for the transcription of the IFN-γ gene [26]. On the basis of these premises, we analyzed the impact of inhibition of TPL2 kinase activity on αGalCer-induced transcription factor engagement in DN32.D3 cells. The results showed that TPL2 is required for αGalCer-mediated upregulation of JunB (Fig. 3A) and the nuclear translocation of NFAT (Fig. 3B).

ERK has been implicated in upregulation of JunB in response to CD30 ligation (35) and the PI3K-Akt signaling pathway inhibits GSK3β, the protein kinase that phosphorylates NFAT and promotes its export from the nucleus [27].

Research Article doi: 10.18081/2333-5106/015-01/339-356

Because TPL2 is required for the activation of both ERK and Akt signals in αGalCer-stimulated iNKT cells (Fig. 3D, 3G), we analyzed the effect of UO126 and wortmannin on JunB upregulation and NFAT localization, respectively. As shown in Fig. 3A, inhibition of the MEK/ERK axis leads to a profound reduction in αGalCer-induced *junB* mRNA levels, similar to the effect of TPL2 inhibitor treatment. Immunoblot analysis of nuclear protein extracts isolated from αGalCer-stimulated DN32.D3 cells revealed a dramatic reduction in NFAT levels following TPL2 or wortmannin inhibitor (Fig. 3B). We conclude that the *ifng* and *il4*-regulating transcription factors JunB and NFAT are targets of the TPL2/ERK and TPL2/Akt signaling pathways, respectively (Fig.3C).

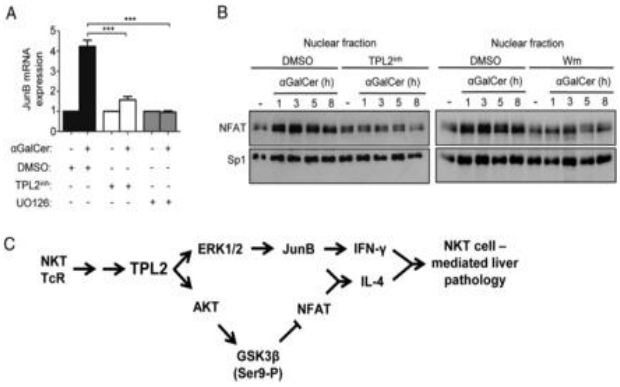

Figure 3.

TPL2 signal transduction targets JunB and NFAT following NKT cell activation. (**A**) Quantitative real-time PCR for JunB expression in DN32.D3 cells treated with TPL2 inhibitor, UO126, or vehicle control (DMSO) followed by αGalCer stimulation for 5 h.

TPL2 kinase activity is required for IL-4 and IFN-γ gene expression in iNKT cells by regulating ERK and Akt signals

To gain insight into the mechanism by which TPL2 influences pathogenic iNKT cell functions, we have explored αGalCer-induced signal transduction in the mouse NKT hybridoma cell line DN32.D3 engineered to express CD1d [28]. αGalCer-stimulated DN32.D3 cells express IL-2 and upregulate genes (*Il4*, *Il10*, and *Ifng*) encoding cytokines that define classic iNKT cells [29]. Treatment of DN32.D3 cells with TPL2 kinase inhibitor prior to αGalCer stimulation led to a dramatic reduction in secreted IL-2 (Fig. 4A) in the absence of an effect on cell viability (data not shown). This treatment also led to reduced IL-4 secretion (Fig. 4A) and *il4* mRNA expression (Fig. 4B) and intracellular IL-4 protein levels (Fig. 8C). Similar results were obtained for IFN-γ expression (Fig. 4A, 4B), mirroring the effects of TPL2 ablation on αGalCer responses in vivo and in primary cultures.

Research Article doi: 10.18081/2333-5106/015-01/339-356

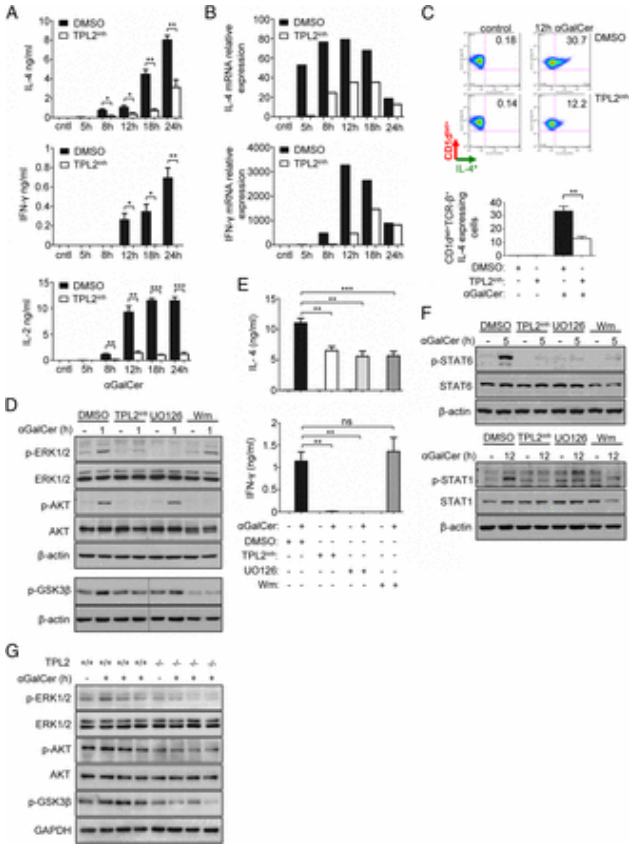

FIGURE 4.
TPL2 regulates ERK1/2, Akt, STAT1, and STAT6 signaling and modulates NKT cell–associated cytokine production following NKT cell activation. (**A**) Culture supernatants of DN32.D3 cells treated with TPL2 inhibitor or vehicle control (DMSO) in the presence or absence of αGalCer were collected and analyzed for production of the NKT cell–associated cytokines IL-4, IFN-γ, and IL-2 by ELISA. Results are representative of three independent experiments; *$p < 0.05$, **$p < 0.01$, ***$p < 0.001$. (**B**) Quantitative real-time PCR for IL-4 and IFN-γ mRNA in DN32.D3 cells treated with TPL2 inhibitor in the presence or absence of αGalCer. A representative graph of three independent experiments, each performed in duplicate, is shown. (**C**) DN32.D3 cells were stimulated with αGalCer and TPL2 inhibitor or vehicle control for 12 h.

TPL2 ablation ameliorates immune-mediated liver injury

The physiological role of TPL2 in immune-mediated liver injury was explored using an established mouse model of fulminant hepatitis-like pathology induced by Con A [28]. Wild-type (WT; *tpl2*$^{+/+}$) and TPL2-deficient (*tpl2*$^{-/-}$) mice were administered Con A i.v., and disease severity was monitored over time. WT animals progressively developed congestive livers characterized by increased blood accumulation (Fig. 5A), histological manifestations of extensive tissue damage (Fig. 5B), and elevated expression of cleaved caspase-3 (Fig. 5C, 5D). Strikingly, *tpl2*$^{-/-}$ mice exposed to Con A displayed reduced macroscopic and histological features of liver injury (Fig. 5A–D). The serum levels of ALT and AST, which represent biochemical markers of hepatic injury (Fig. 5E) and of the proinflammatory cytokines TNF-α and IL-6 (Supplemental Fig. 5A) as markers of systemic effects, were also significantly reduced in *tpl2*$^{-/-}$ compared with WT mice treated with Con A. Con A also led to accumulation of TPL2 mRNA and protein levels in the liver of WT animals (Fig. 5F, 5G).

Research Article doi: 10.18081/2333-5106/015-01/339-356

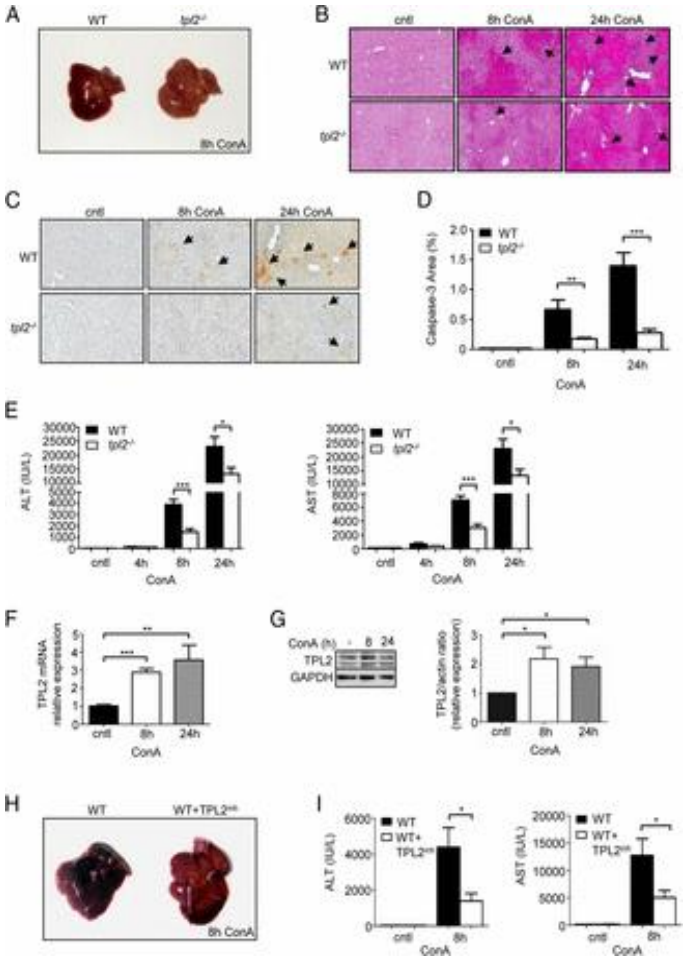

FIGURE 5.
TPL2 kinase promotes immune-mediated liver injury. (**A**) Representative images of livers of WT and *tpl2*$^{-/-}$ mice treated with 10 mg/kg Con A for 8 h showing macroscopic signs of severe and mild liver injury, respectively. (**B**) Histopathological examination of Con A–induced liver injury following H&E staining of liver sections. Arrows show large inflamed and necrotic areas. (**C**) Representative (n = 8) immunohistochemical analysis of cleaved caspase-3 levels in livers from WT and *tpl2*$^{-/-}$ mice treated with saline or Con A for 8 and 24 h. Arrows indicate areas of massive hepatocyte apoptosis positive for cleaved caspase-3 (original magnification ×100). (**D**) Graph represents quantification of cleaved caspase-3 staining in liver sections of WT and *tpl2*$^{-/-}$ mice treated with saline or Con A for 8 and 24 h. Morphometric image analysis was performed using Leica QWin software. (Data are expressed as the mean ± SEM of n = 8 mice/time point; $^{**}p < 0.01$, $^{***}p < 0.001$.) (**E**) Serum ALT and AST levels 4, 8, and 24 h after injection of saline or Con A in WT and *tpl2*$^{-/-}$ mice.

Discussion

Apoptosis has been implicated as a modality of cell death in multiple models [1]. Some examples include *in vitro* exposure of rat hepatocytes to the human bile acid glycochenodeoxycholate, which results in prototypical apoptosis that is preventable by caspase inhibitors [29]. Additionally, galactosamine/endotoxin treatment in mice causes TNF-α dependent apoptosis and inflammatory liver injury that is also effectively prevented when caspase inhibitors are given before the onset of apoptosis [30].

Research Article doi: 10.18081/2333-5106/015-01/339-356

Similarly, activation of the Fas receptor by either an agonistic antibody or Fas ligand triggers hepatocellular apoptosis that can be completely prevented by caspase inhibitors [5,12]. While there are a number of other models that have been suggested to be apoptotic in nature, many of these studies are controversial in their analysis of the data [31].

The bile duct ligation model of cholestasis does not result in activation of caspases or histological apoptosis; the injury is caused primarily by inflammatory necrosis mediated by neutrophils [32]. Similarly, hepatic ischemia reperfusion injury does not involve caspase activation and morphological evidence of apoptosis [33]. In both cases, caspase inhibitors do not protect against the injury [34]. Likewise, acetaminophen (APAP)-induced liver injury in mice cannot be attenuated by caspase inhibitors [35].

Although there is evidence of modest caspase activation in human patients with APAP hepatotoxicity [36], obstructive cholestasis [37], and alcoholic hepatitis [18], the pathophysiological relevance is likely minor and thus, caspase inhibitors may not have a major impact on the pathophysiology. A case in point was the use of the pan-caspase inhibitor IDN-6556 to attenuate reperfusion injury in human liver transplants. The inhibitor was only effective when added to the storage solution but not when administered during reperfusion, i.e. at the time of the assumed apoptotic cell death [38].

This raised the concern that the effects of high concentrations of the caspase inhibitor were due to off-target effects, i.e. inhibition of other proteases such as calpains and cathepsins during ischemia, rather than inhibition of apoptosis during reperfusion. The recently developed M65/M30 ELISA kits that use differential cleavage of keratin-18 by caspases to determine apoptotic versus non-apoptotic cell death conclusively demonstrated that while there is detectable apoptosis in APAP-induced or cholestatic liver injury in human patients, the level of non-apoptotic cell death commonly exceeds these values by ratios of 10:1 or greater [39]. Even in diseases with some degree of apoptosis, other therapeutic options are commonly present, and may be more efficacious.

Hepatitis C is a disease where there are definitive increases in apoptosis in patients, although individual Hepatitis C proteins can have varying effects on apoptosis in different experimental models [40]. Despite this well-defined characteristic, caspase inhibitors as a therapeutic option are probably unwarranted at this juncture.

Not only would it require chronic therapy, but newer direct-acting antivirals can actively destroy the virus by targeting non-structural proteins. This class of drugs has been largely curative, and thus while apoptosis may have once been a solid therapeutic target, it is unlikely it will have additional substantial curative benefit, even in difficult to cure genotypes. As such, the primary issues facing the current Hepatitis C burden are optimizing treatment regimens of the new direct-activing antiviral drugs and reaching sick and at-risk patient populations for early detection [41].

Research Article doi: 10.18081/2333-5106/015-01/339-356

Thus, it is critical to objectively assess the importance and the relevance of apoptotic cell death in a given pathophysiology, especially in humans, before the therapeutic use of caspase inhibitors is considered.

A functional link between TPL2 and iNKT cell–mediated pathology was inferred by the observation that TPL2 is required for the accumulation of $CD3^+NK1.1^+$ NKT cells in the liver and the development of fulminant hepatitis in mice exposed to Con A. Although NKT cells are phenotypically diverse, we have focused on $CD3^+NK1.1^+$ NKT cells given their established pathogenic role in liver injury in C57BL/6 mice [38]. Increased numbers of hepatic NKT cells have been documented in patients with autoimmune liver diseases [13] and genetic ablation of NKT cells in the mouse alleviates the deleterious effects of Con A on liver injury [11]. Activated iNKT cells produce large amounts of the effector cytokines IFN-γ and IL-4 that play important roles in Con A–induced liver pathology by mediating hepatocyte killing [25] and neutrophil infiltration [22], respectively.

Data presented in this study show that TPL2 regulates hallmarks of iNKT cell activation in vivo, as evidenced by the reduction in circulating levels of IL-4 and IFN-γ and in hepatic accumulation of neutrophils in Con A–treated *tpl2*$^{-/-}$ mice. In line with these associations, the adoptive transfer of *tpl2*$^{-/-}$ NKT cells in NKT cell–deficient animals were largely ineffective in restoring susceptibility to the disease compared with that of TPL2-proficient NKT cells. However, the observation that TPL2 ablation alleviates but does not abolish Con A–mediated liver injury indicates the operation of additional kinase pathways controlling immune-mediated hepatitis in this mouse model.

iNKT cells respond to glycolipid Ags presented by CD1d on APCs, including αGalCer [21]. Mice immunized with αGalCer undergo mild hepatitis associated with elevated levels of liver transaminases and proinflammatory cytokines, IL-4–dependent neutrophil infiltration and induction of hepatocyte killing [32]. TNF-α and IFN-γ have been identified as important mediators of hepatic injury in this model, an effect mediated by increased expression of Fas ligand (CD178) in iNKT cells [40]and Fas (CD95) and STAT1-IFN regulatory factor 1 in affected hepatocytes [41].

Data presented in this paper demonstrate that TPL2 ablation alleviates the aforementioned pathogenic effects of the iNKT-specific ligand αGalCer in vivo, including TNF-α synthesis, and reduces IL-4 and IFN-γ production in primary splenocyte and LMNC cultures. Using a coculture system of *tpl2*$^{+/+}$ and *tpl2*$^{-/-}$ DCs and NKT cells, we have excluded defects in αGalCer presentation by DCs as drivers of reduced effector cytokine synthesis by *tpl2*$^{-/-}$ iNKT cells (Fig. 6C). Collectively, these observations directly link TPL2 to pathogenic iNKT cell function.

The profound protective outcomes of TPL2 ablation in experimental models of fulminant (Con A) and mild (αGalCer) hepatitis discussed above, coupled with the absence of an effect on iNKT cell development, highlight TPL2 as putative target for the management of immune-driven liver pathology.

Research Article doi: 10.18081/2333-5106/015-01/339-356

In line with this concept, administration of a TPL2 kinase inhibitor attenuates the pathological manifestations of experimental hepatitis in vivo and the production of IFN-γ and IL-4 by iNKT cells in vitro.

Thus, further studies are warranted to evaluate the potential of TPL2 kinase inhibitors to minimize the severity of inflammatory liver diseases and their comorbidities.

Which are the molecular pathways that link TPL2 to effector cytokine synthesis in NKT cells? The physiological role of TPL2 in signal transduction has largely been explored downstream of Toll-like and TNF receptors in macrophages, dendritic, and hepatic stellate cells [41]. These studies have shown that TPL2 ablation ameliorates ERK activation and renders macrophages defective in the production of TNF and other proinflammatory molecules [42]. Data presented in this paper demonstrate that TPL2 is required for ERK signaling also downstream of the iNKT TCR. We show that signals transduced via the TPL2-ERK pathway regulate the transcription factor JunB, which controls the expression of the IFN-γ gene in iNKT cells and influences αGalCer-induced inflammatory liver disease in the mouse [43]. Our findings also uncover a novel physiological role for TPL2 in Akt activation and show that this signaling axis promotes the nuclear accumulation of NFAT in αGalCer-challenged iNKT cells.

Pertinent to these observations, the NFAT:JunB complex represents a major component of the *il4* transcriptional machinery [44]. Therefore, TPL2 coordinates effector cytokine synthesis in NKT cells via ERK- and Akt-transduced signals.

An important aspect of TPL2 signaling is its interplay with regulators of the NF-κB pathway such as the IKKβ, which is required for TPL2 activation downstream of TLR4 and TNFR1 [45].

Data presented in this paper show that αGalCer-challenged iNKT cells engage TPL2-dependent ERK signaling in the absence of an effect on the NF-κB path. It is thus conceivable that alternative mechanisms may operate to regulate TPL2 signal transduction downstream of the iNKT TCR, a hypothesis that merits further investigations. The existence of alternative mechanism(s) of TPL2 activation is supported by a recent study describing TPL2-dependent but IKKβ-independent activation of ERK during TLR3 and TLR9 signaling in macrophages [46].

Conclusion

The protective effects of TPL2 ablation or inhibition of its kinase activity on hepatic inflammation may have important ramifications for the development of therapies for liver diseases. Given the capacity of iNKT cells to orchestrate the licensing and activation of other immune cells, our results may also help to better appreciate the diverse and often contradictory effects of TPL2 on immune functions.

Research Article doi: 10.18081/2333-5106/015-01/339-356

Competing interests

The authors declare that they have no competing interests.

References

1. Okajima K, Harada N, Uchiba M. Ranitidine reduces ischemia/reperfusion-induced liver injury in rats by inhibiting neutrophil activation. J Pharmacol Exp Ther 2002;301:1157–1165. [View In Article]
2. Sakakura Y, Kaibori M, Oda M, Okumura T, Kwon AH, Kamiyama Y. Recombinant human hepatocyte growth factor protects the liver against hepatic ischemia and reperfusion injury in rats. J Surg Res 2000;92:261–266. [View In Article]
3. Selzner N, Rudiger H, Graf R, Clavien P. Protective strategies against ischemic injury of the liver. Gastroenterology 2003; 125: 917–936. [PubMed]
4. Vougioukalaki M, Kanellis DC, Gkouskou K, Eliopoulos AG. Tpl2 kinase signal transduction in inflammation and cancer. Cancer Lett 2011; 304(2):80–89. [PubMed]
5. Jaeschke H. Molecular mechanisms of hepatic ischemia-reperfusion injury and preconditioning. Am J Physiol Gastrointest Liver Physiol 2003; 284: G15–G26.
6. Gracia-Sancho J, Villarreal G Jr, Zhang Y, Yu JX, Liu Y, Tullius SG. et al. Flow cessation triggers endothelial dysfunction during organ cold storage conditions: strategies for pharmacologic intervention. Transplantation 2010; 90: 142–149.[PubMed]
7. Caraceni P, Domenicali M, Vendemiale G, Grattagliano I, Pertosa A, Nardo B. et al. The reduced tolerance of rat fatty liver to ischemia reperfusion is associated with mitochondrial oxidative injury. J Surg Res 2005;124:160–168. [Full Text PDF]
8. Tsatsanis C, Patriotis C, Bear SE, Tsichlis PN. The Tpl-2 protooncoprotein activates the nuclear factor of activated T cells and induces interleukin 2 expression in T cell lines. Proc Natl Acad Sci USA 1998; 95(7):3827–3832. [PMC free article] [PubMed]
9. Hessheimer AJ, Fondevila C, Taurá P, Muñoz J, Sánchez O., Fuster J. et al. Decompression of the portal bed and twice-baseline portal inflow are necessary for the functional recovery of a “small-for-size” graft. Ann Surg 2011; 253: 1201–1210. [PubMed]
10. Schlegel A, Rougemont O, Graf R, Clavien PA, Dutkowski P. Protective mechanisms of end-ischemic cold machine perfusion in DCD liver grafts. J Hepatol 2013; 58: 278–286. [PubMed]
11. Schiesser M, Wittert A, Nieuwenhuijs VB, Morphett A, Padbury RT, Barritt GJ. Intermittent ischemia but not ischemic preconditioning is effective in restoring bile flow after ischemia reperfusion injury in the livers of aged rats. J Surg Res 2009; 152: 61–68. [PubMed]
12. Esposti DD, Domart MC, Sebagh M, Harper F, Pierron G, Brenner C. et al. Autophagy is induced by ischemic preconditioning in human livers formerly treated by chemotherapy to limit necrosis. Autophagy 2010; 6: 172–174. [PubMed]
13. Serracino-Inglott F, Habib NA, Mathie RT. Hepatic ischemia-reperfusion injury. Am J Surg 2001;181:160–166. [Full Text]
14. Clemens MG. Nitric oxide in liver injury. Hepatology 1999; 30: 1–5. [Scopus] [PubMed]
15. Jaeschke H. Molecular mechanisms of hepatic ischemia-reperfusion injury and preconditioning. Am J Physiol Gastrointest Liver Physiol 2003; 284: G15-G26. [PubMed]
16. Parmar KM, Larman HB, Dai G, Zhang Y, Wang ET, Moorthy SN, et al. Integration of flow-dependent endothelial phenotypes by Kruppel-like factor 2. J Clin Invest 2006; 116: 49-58. [PubMed]
17. Imamura H, Brault A, Huet PM. Effects of extended cold preservation and transplantation on the rat liver microcirculation. Hepatology 1997; 25: 664–671. [PDF(316K)]
18. Guarrera JV, Estevez J, Boykin J et al. Hypothermic machine perfusion of liver grafts for transplantation: Technical development in human discard and miniature swine models. Transplant Proc 2005; 37: 323–325. [CrossRef] [PubMed]
19. Lee CY, Zhang JX, Jones JW Jr, Southard JH, Clemens MG. Functional recovery of preserved livers following warm ischemia: Improvement by machine perfusion preservation. Transplantation 2002; 74: 944–951. [PubMed]

20. Shinoda M , Shimazu M , Matsuda S et al. c-Jun N-terminal kinase activation during warm hepatic ischemia/reperfusion injuries in a rat model . Wound Repair Regen 2002 ; 10 : 314 – 319. [Full Article (HTML)]
21. St Peter SD, Imber CJ, Lopez I, Hughes D, Friend PJ. Extended preservation of non-heart-beating donor livers with normothermic machine perfusion. Br J Surg 2002; 89: 609–616. [Abstract]
22. Imber CJ, St Peter SD, Lopez de Cenarruzabeitia I, Pigott D, James T, Taylor R, et al. Advantages of normothermic perfusion over cold storage in liver preservation. Transplantation 2002; 73: 701–709. [PubMed]
23. Lauschke H, Olschewski P, Tolba R, Schulz S, Minor T. Oxygenated machine perfusion mitigates surface antigen expression and improves preservation of predamaged donor livers. Cryobiology 2003; 46: 53–60. [PubMed]
24. Abu-Amara M, et al. Liver ischemia/reperfusion injury: Processes in inflammatory networks—a review. Liver Transpl 2010;16:1016–1032. [PubMed]
25. Selzner N, Rudiger H, Graf R, Clavien PA. Protective strategies against ischemic injury of the liver. Gastroenterology 2003;125:917–936. [PubMed]
26. Shen XD, et al. Inflammatory responses in a new mouse model of prolonged hepatic cold ischemia followed by arterialized orthotopic liver transplantation. Liver Transpl 2005;11:1273–1281. [PubMed]
27. Land WG. The role of postischemic reperfusion injury and other nonantigen-dependent inflammatory pathways in transplantation. Transplantation. 2005;79:505–514. [PubMed]
28. Srikrishna G, Freeze HH. Endogenous damage-associated molecular pattern molecules at the crossroads of inflammation and cancer. Neoplasia. 2009;11:615–628. [PMC free article] [PubMed]
29. Kawai T, Akira S. Toll-like receptor and RIG-I-like receptor signaling. Ann NY Acad Sci. 2008;1143:1–20. [PubMed]
30. Takeuchi O, Akira S. Pattern recognition receptors and inflammation. Cell 2010;140:805–820. [PubMed]
31. Akira S, Takeda K. Toll-like receptor signalling. Nat Rev Immunol 2004;4:499–511. [PubMed]
32. Pulskens WP, et al. Toll-like receptor-4 coordinates the innate immune response of the kidney to renal ischemia/reperfusion injury. PLoS ONE. 2008;3:e3596. [PMC free article] [PubMed]
33. Kaczorowski DJ, et al. Mechanisms of Toll-like receptor 4 (TLR4)-mediated inflammation after cold ischemia/reperfusion in the heart. Transplantation. 2009;87:1455–1463. [PMC free article] [PubMed]
34. Shigeoka AA, et al. TLR2 is constitutively expressed within the kidney and participates in ischemic renal injury through both MyD88- dependent and -independent pathways. J Immunol 2007;178:6252–6258. [PubMed]
35. Ren F, et al. Inhibition of glycogen synthase kinase 3 beta ameliorates liver ischemia reperfusion injury by way of an interleukin-10-mediated immune regulatory mechanism. Hepatology 2011;54:687–696. [PMC free article] [PubMed]
36. Dumitru CD, et al. TNF-alpha induction by LPS is regulated posttranscriptionally via a Tpl2/ERK-dependent pathway. Cell. 2000;103(7):1071–1083. [PubMed]
37. Fiorini RN, et al. Anti-endotoxin monoclonal antibodies are protective against hepatic ischemia/reperfusion injury in steatotic mice. Am J Transplant 2004;4:1567–1573. [PubMed]
38. Bamboat ZM, et al. Toll-like receptor 9 inhibition confers protection from liver ischemiareperfusion injury. Hepatology 2009; 51:621–632. [PMC free article] [PubMed]
39. Huang H, et al. Endogenous histones function as alarmins in sterile inflammatory liver injury through Toll-like receptor 9 in mice. Hepatology 2011; 54:999–1008. [PMC free article] [PubMed]
40. Cavassani KA, et al. TLR3 is an endogenous sensor of tissue necrosis during acute inflammatory events. J Exp Med 2008; 205:2609–2621. [PMC free article] [PubMed]
41. Kariko K, Ni H, Capodici J, Lamphier M, Weissman D. mRNA is an endogenous ligand for Toll-like receptor 3. J. Biol. Chem 2004; 279:12542–12550. [PubMed]

Research Article doi: 10.18081/2333-5106/015-01/339-356

42. Bone RC, Sibbald WJ, and Sprung CL. The ACCP-SCCM consensus conference on sepsis and organ failure. Chest 1992; 101:1481–1483. [PubMed]
43. Jiang W, Sun R, Wei H, Tian Z. Toll-like receptor 3 ligand attenuates LPS-induced liver injury by down-regulation of toll-like receptor 4 expression on macrophages. Proc. Natl. Acad. Sci. USA. 2006;102:17077–17082. [PMC free article] [PubMed]
44. Wornle M, Schmid H, Banas B, Merkle M, Henger A, Roeder M, Blattner S, Bock E, Kretzler M, Grone HJ, Schlondorff D. Novel role of toll-like receptor 3 in hepatitis C-associated glomerulonephritis. Am. J. Pathol 2006;168:370–385. [PMC free article] [PubMed]
45. Tabiasco J, Devevre E, Rufer N, Salaun B, Cerottini JC, Speiser D, Romero P. Human effector CD8+ T lymphocytes express TLR3 as a functional coreceptor. J. Immunol 2006;177:8708–8713. [PubMed]
46. Yun Y, Zheng X, Chen L,Su Y, Kim C, Zhao M. Expression of ATF3 in mouse protects the liver against sepsis via inhibiting HMGB expression. American Journal of BioMedicine 2014; 2(3):337-349. [Abstract]